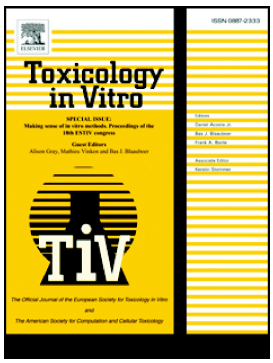

Acute effects of lead on porcine neonatal Sertoli cells in vitro

Francesca Mancuso, Iva Arato, Cinzia Lilli, Catia Bellucci, Maria Bodo, Mario Calvitti, Maria Chiara Aglietti, Marco dell'Omo, Claudio Nastruzzi, Riccardo Calafiore, Giovanni Luca, Lorella Marinucci

PII: S0887-2333(17)30379-X
DOI: https://doi.org/10.1016/j.tiv.2017.12.013
Reference: TIV 4190

To appear in: *Toxicology in Vitro*

Received date: 23 August 2017
Revised date: 17 November 2017
Accepted date: 18 December 2017

Please cite this article as: Francesca Mancuso, Iva Arato, Cinzia Lilli, Catia Bellucci, Maria Bodo, Mario Calvitti, Maria Chiara Aglietti, Marco dell'Omo, Claudio Nastruzzi, Riccardo Calafiore, Giovanni Luca, Lorella Marinucci , Acute effects of lead on porcine neonatal Sertoli cells in vitro. The address for the corresponding author was captured as affiliation for all authors. Please check if appropriate. Tiv(2017), https://doi.org/10.1016/j.tiv.2017.12.013

ACUTE EFFECTS OF LEAD ON PORCINE NEONATAL SERTOLI CELLS IN VITRO

Running title: EFFECTS OF LEAD ON SERTOLI CELLS

Francesca Mancuso[a,*], Iva Arato[a], Cinzia Lilli[a], Catia Bellucci[a], Maria Bodo[a], Mario Calvitti[a], Maria Chiara Aglietti[b], Marco dell'Omo[b,c], Claudio Nastruzzi[d], Riccardo Calafiore[b,e], Giovanni Luca[a,e§], Lorella Marinucci[a§]

[a]Department of Experimental Medicine and Biochemical Sciences, University of Perugia, Perugia, 06132, Italy

[b]Department of Medicine, University of Perugia, Perugia, 06132, Italy

[c]Section of Occupational Medicine, Respiratory Diseases and Toxicology, University of Perugia, 06132, Italy

[d]Department of Life Sciences and Biotechnology, University of Ferrara, Ferrara, 44121, Italy;

[e]Division of Medical Andrology and Endocrinology of Reproduction, Saint Mary Hospital, Terni, 05100, Italy;

§Share senior authorship to this paper

CORRESPONDING AUTHOR AND REPRINT REQUEST:

Dr. Francesca Mancuso

Department of Experimental Medicine

Piazzale L. Severi.

University of Perugia

06132, Perugia, Italy.

Tel: +390755858232

e-mail: francesca.mancuso@unipg.it

Key words: Sertoli cells, lead acetate, toxicity.

Abbreviations

3β–HSD: 3β-Hydroxysteroid dehydrogenase

AKT: protein kinase B

AMH: anti-Müllerian hormone

ASMA: anti-smooth muscle antibody

ECL: enhanced chemiluminescence

ERK1/2: extracellular signal-regulated kinase 1/2

FSH: follicle stimulating hormone

FSH-r: follicle stimulating hormone receptor

ITS: insulin-transferrin-selenium

JNK: c-Jun N-terminal kinase

MAPK: Mitogen Activated Protein Kinase

MTT: 3-(4,5-dimethylthiazolyl-2)-2,5-diphenyltetrazoliumbromide

NaCl: sodium chloride

OSHA: occupational safety and health administration

RIPA: radioimmunoprecipitation assay buffer

SCs: Sertoli cells

WB: western blotting

Abstract

Environmental pollution is one of the main factors responsible for reducing fertility in males. Lead is one of the major heavy metal contaminants that impairs several organs; it preferentially accumulates in male reproductive organs and alters sperm quality both *in vivo* and *in vitro*. However, the underlying mechanisms remain unclear. Sertoli cells (SCs) provide structural and physiological support to spermatogenic cells within seminiferous tubules. Therefore, changes in SCs affect the developing germ cells and alter spermatogenesis. This study aimed to assess whether exposure to subtoxic doses of adversely affects SC functioning in higher mammals. Purified and functional porcine neonatal SCs were exposed to lead acetate at three different concentrations. Lead exposure decreased the mRNA expression and protein levels of inhibin B and anti-Mullerian hormone (AMH) compared to control, indicating loss of FSH-r integrity in terms of 17-β-oestradiol production under FSH stimulation. In addition, we observed an increase in the mRNA levels of Akt and mTOR, and the phosphorylation of p38 and Akt in SCs exposed to lead at all concentrations compared to unexposed control SCs. In conclusion, lead is toxic to SCs, even at low concentrations, and is expected to alter spermatogenesis.

1. Introduction

Environmental pollution is a serious worldwide health concern. Major pollutants include heavy metals, such as lead (Vaseem et al, 2017), mercury (Obrist et al, 2017), and cadmium (Luca et al, 2013, Bodo et al, 2010, Baroni et al, 2015), as well as tobacco smoke (Marinucci et al, 2014); they have been widely studied in recent decades because of their adverse effects on living organisms. Lead affects the functioning of a variety of cells, including those of the nervous system (Mason et al, 2014), the microvascular endothelium (Vaziri, 2008), the kidney (Benjelloun et al, 2007), and the immune system (Dietert et al, 2007). Moreover, lead exposure causes toxic effects on the male reproductive system.

Exposure concentrations up to 10 µM have been reported in the human seminal plasma; particularly, it impairs mammalian spermatogenesis and sperm quality *in vivo*, and inhibits sperm functions *in vitro* (Gidlow, 2004; Pant et al, 2014; Wang et al, 2006). Severe atrophic changes with interstitial cell hyperplasia, SC hyperplasia, tubular atrophy, and sclerosis have been observed in the testicular biopsies of men occupationally exposed to inorganic lead. Histopathological signs of oligospermia, azoospermia, low sperm motility, and a high percentage of abnormal sperms were observed in all the subjects in previous studies (Monsees et al, 2000, Vigeh et al, 2011).

Although unfavourable effects on the reproductive system usually occur at relatively high levels of lead, exposure to lower doses for longer time periods may also similarly alter the male reproductive system (OSHA, 2004). Therefore, occupational health surveillance must include the assessment of adverse effects on the reproductive system of people exposed to subtoxic concentrations of lead.

SCs provide structural and metabolic support to spermatogenic cells within seminiferous tubules (França et al, 2016); therefore, changes in SC functioning may affect the developing germ cells and alter spermatogenesis. Lead induces morphological changes in SCs (Vigeh et al, 2011), alters cell junctions (Adhikari et al, 2000), and causes mitochondrial damage (Li et al, 2016) in rodents. However, mechanisms underlying the toxic effects of lead on SCs in higher mammals remain unexplored, and it is worthwhile to investigate associated signalling pathways.

In mammalian cells, mitogen-activated protein kinases (MAPKs), including ERK (Extracellular Signal-Regulated Kinases), C-Jun N-terminal kinase/stress activated protein kinase (JNK/SAPK), and p38 kinase, have been shown to regulate extracellular signal transduction. By relaying, amplifying, and integrating signals from a diverse range of stimuli, MAPK pathways regulate mammalian cell proliferation, differentiation, development, and apoptosis as well as elicit inflammatory responses (Zhang an d Liu, 2002).

Protein kinase B (Akt) is an anti-apoptotic Ser/Thr kinase; it regulates insulin signalling and glucose metabolism by modulating the effects of insulin on target cells (Zhang et al, 2012). Moreover, Eckers and Klotz (2009) reported that copper [Cu(II)] or zinc [Zn(II)] activates the PI3K (phosphatidylinositol 3-kinase)/Akt signalling cascade in the presence of stressful stimuli in the cells of mammals or *Caenorhabditis elegans*, thereby exhibiting insulin-mimetic effects on cell proliferation. Moreover, Ser/Thr kinase mammalian target of rapamycin (mTOR), a potential downstream effector of the PI3K pathway, controls key cellular processes, such as cell survival, growth, and proliferation (Dowling et al, 2010). Based on these reports, the aim of the present *in vitro* study was to assess the effects of sub-toxic lead exposure on the viability and functioning of purified pig neonatal SCs (Luca et al, 2015), and to identify underlying signalling pathways.

2. Materials and methods

2.1. Isolation, purification, and morphological characterisation of SCs

All animal studies were conducted in agreement with the guidelines adopted by the Italian Approved Animal Welfare Assurance (A-3143-01) and the University of Perugia Animal Care and Use Committee. The experimental protocols were approved by the University of Perugia. Neonatal Large White pigs, aged 7–15 days, were used as SC donors. SCs were isolated according to previously established methods after slight modifications (Luca et al, 2015).

Immunostaining for markers of SCs [anti-Mullerian hormone (AMH) and vimentin], Leydig cells [3β-hydroxysteroid dehydrogenase (3β-HSD)], and peritubular cells [anti-smooth muscle antibody (ASMA)] were performed according to previously established methods with minor changes (Luca et al, 2007, Luca et al, 2015).

SC monolayers were morphologically characterised after lead exposure by fluorescence microscopy with a phalloidin conjugates that reacts with the actin cytoskeleton of cells. Briefly, lead-exposed SC monolayers were grown on glass chamber slides (LabTek II, Nunc, Thermo Fisher, Rochester, NY, USA), and fixed in 4% PFA-PBS for 15 min. The fixed cells were then permeabilised (PBS, 0.2% Triton X-100) for 10 min at room temperature, and blocked with 0.5% BSA (Sigma-Aldrich, St. Louis, MO, USA) in PBS for 1 h prior to exposure to phalloidin Alexa Fluor 555 (A4-055, Molecular Probes, OR, USA; dilution factor, 1:50) at room temperature for 1 h. Thereafter, the cells were treated with RNAse (10 mg/mL, Sigma-Aldrich) and counterstained for 1 min with DAPI (Sigma-Aldrich). The cells were mounted with ProLong® Gold antifade reagent (Molecular Probes, NY, USA). The morphology of lead-exposed SCs was visualized under a BX-41 microscope (Olympus, Tokyo, Japan) equipped with a fluorescence camera (F-viewer, Olympus); images were processed with the Cell F imaging software (Olympus).

2.2. SC culture and lead exposure

SCs were maintained at 37°C and 5% CO_2 in the absence (unexposed) or presence of lead acetate (Sigma-Aldrich) at concentrations of 10, 20, and 40 µM in HAMF12 (Euroclone, Milan, Italy) supplemented with 0.166 nM retinoic acid (Sigma-Aldrich) and 5 mL/500 mL of Insulin-Transferrin-Selenium (ITS) (Cat. No. 354352; Becton Dickinson, NJ, USA) for 48 h.

2.3. Follicle stimulating hormone receptor (FSH-r) functional integrity

We assessed FSH-r integrity on the surfaces of SCs by measuring 17-β-oestradiol production under FSH stimulation with or without testosterone by using an ELISA kit (ALPCO Immunoassay, Salem, USA; intra-assay CV<4.0%; inter-assay CV<8.0%) as previously described (Luca et al, 2013).

2.4. Inhibin B and AMH secretion assay

Aliquots of the culture media of unexposed and lead-exposed SCs were collected, stored at -20°C for the assessment of inhibin B (Inhibin B Gen II ELISA, Beckman Coulter, Webster, TX, USA; intra-assay CV=2.81%; inter-assay CV=4.33%) and AMH (AMH Gen II ELISA, Beckman Coulter; intra-assay CV=3.89%; inter-assay CV=5.77%) secretion as previously described (Giovagnoli et al, 2014).

2.5. Western blot (WB) analysis

After collecting the supernatants, unexposed and lead-exposed SC monolayers were scraped off to obtain whole-cell extracts. Briefly, the cells were resuspended in 100 µL of radioimmunoprecipitation assay lysis buffer (Santa Cruz Biotechnology Inc., Santa Cruz, CA, USA). After centrifuging the mixture at 1,000 ×*g* (Eppendorf, NY, USA) for 10 min, the supernatant was collected, and total protein content was determined by the Bradford method (Bradford, 1976). Sample aliquots were stored at -20°C for WB analysis.

The cell extracts were separated by 4–12% SDS-PAGE, and equal amounts of protein (70 µg protein/lane) were run and blotted on nitrocellulose membranes (BioRad, Hercules, CA, USA). The membranes were incubated overnight in a buffer containing 10 mM TRIS, 0.5 M NaCl, 1% (v/v) Tween 20 (Sigma-Aldrich), rabbit anti-ERK1/2 (Millipore, MA, USA; dilution factor, 1:2000), mouse anti-phospho-ERK1/2 (Millipore; dilution factor, 1:100), rabbit anti-JNK (Millipore; dilution factor, 1:1000), rabbit anti-phospho-JNK (Millipore; dilution factor, 1:500), mouse anti-p38 (Millipore; dilution factor, 1:2000), rabbit anti-phospho-p38 (Millipore; dilution factor, 1:2000), rabbit anti-Akt (Cell Signalling; dilution factor, 1:100), rabbit anti-phospho-Akt (Cell Signalling; dilution factor, 1:1000), and mouse anti-actin (Sigma-Aldrich; dilution factor, 1:100) primary antibodies. Primary antibody binding was then detected by incubating the membranes for an additional 60 min in a buffer containing horseradish peroxidase-conjugated anti-rabbit (Sigma-Aldrich; dilution factor, 1:5000), anti-

goat (Santa Cruz Biotechnology Inc.; dilution factor, 1:5000), and/or anti-mouse (Santa Cruz Biotechnology Inc.; dilution factor, 1:5000) IgG secondary antibodies. The bands were detected by enhanced chemiluminescence.

2.6. RT-PCR analysis

Total RNA was isolated from unexposed and Lead-exposed SC monolayers using an RNA purification kit (Versagene RNA Cell Kit, Gentra Systems, Minneapolis, MN, USA), and quantified by reading the optical density at 260 nm. Thereafter, 1 µg of total RNA was diluted to a final volume of 20 µL and reverse transcribed by the Maxima First Strand cDNA Synthesis kit (Thermo Scientific, MA, USA). RT-PCR was performed after mixing 16 ng of the prepared cDNA with the SYBR Green reagent (Stratagene, Amsterdam, Netherlands) in an Mx3000P cycler (Stratagene) using FAM for detection and ROX as the reference dye. The mRNA level of each gene was normalized against that of β-actin, and expressed as fold change relative to unexposed control values; all values were computed with the MxPro QPCR Software (Stratagene, Amsterdam, Netherlands). The sequences of primers used in this study are listed in Table 1.

TABLE 1 Primer sequences for PCR analyses.

Gene	Forward Sequences (5′–3′)	Reverse Sequences (5′–3′)
AMH	GCGAACTTAGCGTGGACCTG	CTTGGCAGTTGTTGGCTTGATATG
Inhibin B	CCGTGTGGAAGGATGAGG	TGGCTGGAGTGACTGGAT
FSH-r	TGAGTATAGCAGCCACAGATGACC	TTTCACAGTCGCCCTCTTTCCC
Akt	CCAACACCTTCATCATCC	AAGTCCATCATCTCTTCCT

m-TOR	CTCTCATCAGCATCAATAATAAG	GGTGTCCATCTTCTTGTC
β-actin	ATGGTGGGTATGGGTCAGAA	CTTCTCCATGTCGTCCCAGT

2.7. Cell number

The number of cells was evaluated by the trypan blue exclusion assay. Detached cells were pelleted by centrifugation at 800 ×*g* for 5 min and mixed with 0.4% trypan blue (Sigma-Aldrich) in a 1:1 ratio; the cells were then counted using an automated cell counter (Invitrogen, CA, USA).

2.8. Cytotoxicity assay

Lead toxicity in SC monolayers was measured using the MTT assay as previously described (Luca et al, 2013). Background and negative control absorbance values were obtained by measuring the absorbance of the blank culture medium (without SCs) and the culture medium of unexposed SCs, respectively. The viability of lead-exposed SCs was expressed as a percentage of viability of unexposed SCs (enzyme activity of lead-exposed SCs×100/enzyme activity of unexposed SCs).

2.9. Statistical analysis

Values reported in the figures are the mean±S.E.M. of three independent experiments, each one performed in triplicate. Statistical analysis was performed by the paired Student's *t*-test using the SigmaStat 4.0 software (Systat Software Inc., CA, USA). All tests were performed in triplicate, and differences were considered statistically significant when $p<0.05$, $p<0.01$ and $p<0.001$.

3. Results

3.1. Morphological characterisation of SCs

The isolated SC culture was 95% pure as indicated by immunostaining for AMH (Fig. 1a) with an extremely low percentage of non-SC cells (<5%) characterised by immunostaining for 3β-HSD (Leydig cells, Fig. 1b) and ASMA (peritubular cells, Fig. 1c).

After 48 h of exposure to sub-toxic concentrations of lead, no changes in the organization of vimentin filaments in SCs were observed; it appeared as a diffuse filamentous network restricted to the long cytoplasmic processes and perinuclear regions, similar to that in unexposed SCs (Fig. 2a–d). Moreover, we did not observe any changes in actin cytoskeletal organization (Fig. 2e–h); both unexposed and lead-exposed SC monolayers exhibited well-developed stress fibres of actin filaments. Cell morphology was confirmed by light microscopy that showed no changes in lead-exposed SC monolayers compared to unexposed SC monolayers (Fig. 2 i–n).

3.2. *FSH-r integrity*

The evaluation of FSH-r integrity on SC surfaces, in terms of 17-β-oestradiol production under basal conditions and under FSH and/or testosterone stimulation, showed that lead exposure significantly decreases FSH-r integrity in SCs. As shown in Fig. 3, differences between unexposed and lead-exposed SCs at 10, 20, and 40 μM lead concentrations WERE -22.15, -23.70, and -22.07%, respectively (*$p<0.05$ at all lead concentrations); differences between lead-exposed FSH- and testosterone-stimulated SCs and lead-exposed unstimulated SCs at 10, 20, and 40 μM lead concentrations WERE -22.83, -22.99, and -28.32%, respectively (*$p<0.05$ at 10 and 20 μM lead concentrations, and **$p<0.001$ at 40 μM lead concentration).

3.3. Inhibin B and AMH secretion assay

Fig. 4a shows the significantly decreased secretion of inhibin B (*$p<0.05$ with -26.64 and -25.78% at 10 and 20 μM lead concentrations, respectively; **$p<0.01$ with -62.69% at 40 μM lead concentration)

and AMH (**p<0.001 with -71.14, -67.74, and -82.94% at 10, 20, and 40 μM lead concentrations, respectively) in lead-exposed SCs compared to unexposed SCs.

Fig. 4b shows the significantly decreased cellular contents of inhibin B (**p<0.001 with -47.66, -69.57, and -80.84% at 10, 20, and 40 μM lead concentrations, respectively) and AMH (**p<0.01 with -56.00, -67.42, and -78.92% at 10, 20, and 40 μM lead concentrations, respectively) in lead-exposed SCs compared to unexposed SCs.

3.4. *WB analysis*

WB analysis showed that exposure to lead at all concentrations increases p38 and Akt phosphorylation compared to unexposed controls (Fig. 5a and 5b); however, it did not alter the phosphorylation of ERK1/2 and JNK (data not shown).

3.5. RT-PCR analysis

Compared with unexposed controls, the gene expression of FSH-r, inhibin B, and AMH was significantly downregulated by 10, 20, and 40 μM lead exposure (Fig. 6). Differences in the mRNA levels of FSH-r were -34.65, -28.44, and -19.84% at 10, 20, and 40 μM lead concentrations, respectively (**p<0.001 at 10 and 20 μM, and *p<0.05 at 40 μM); differences in the mRNA levels of inhibin B were -34.61, -27.23, and -25.16% at 10, 20, and 40 μM lead concentrations, respectively (**p<0.001 at 10 μM, and *p<0.05 at 20 and 40 μM); differences in the mRNA levels of AMH were -19.55 and -24.68 at 10 and 20 μM lead concentrations, respectively (*p<0.05 at both these concentrations).

The gene expression of Akt and mTOR was significantly upregulated by lead exposure. At lead concentrations of 20 and 40 μM, differences in the mRNA levels of Akt were 16.8 and 37.5%,

respectively (*p<0.05) and those in the mRNA levels of mTOR were 60.83 and 78.33%, respectively (**p<0.001) as shown in Fig. 6.

3.6. Cell number

A significant increase in the number of SCs was observed at 20 (13.33%) and 40 μM (20%) lead concentrations compared to unexposed controls (*p<0.05) as shown in Fig. 7a.

3.7. Cytotoxicity assay

The cytotoxicity of different lead concentrations was determined by the MTT assay. A statistically significant increase in the percentage of viable cells was observed in SCs exposed to lead at all concentrations compared to unexposed controls (*p<0.05 with 38.12 and 31.71% at 10 and 20 μM lead concentrations, respectively; **p<0.001 with 41.83% at 40 μM lead concentration) as shown in Fig. 7b.

4. Discussion

Lead is a ubiquitous environmental toxicant that causes harmful effects on several systems, such as the nervous system (Mason et al, 2014), the microvascular endothelium (Vaziri, 2008), the kidney (Benjelloun et al, 2007), and the immune system (Dietert et al, 2007); however, its effects on the male reproductive system are the most significant (Wirth and Mijal, 2010). In previous *in vitro* studies, the effects of acute (48 h) exposure to lead (10–80 μM) have been studied on primary mouse SCs (Batarseh and Brabec, 1986; Adhikari et al, 2000; Li et al, 2016). In the present study, lead concentrations were selected to mimic human seminal plasma levels of 10–40 μM (Gidlow, 2004; Pant et al, 2014; Wang et al, 2006); exposure to lead at 80 μM is reported to induce extensive mitochondrial toxicity, ROS production, and apoptosis as well as inhibit ATP synthesis (Li et al, 2016).

To understand the mechanisms underlying the effects of lead exposure on mammalian SCs with regard to characteristic SC markers (inhibin B and AMH), we examined the effects of subtoxic concentrations of lead exposure on purified neonatal SC monolayers.

In the present study, light microscopy analysis revealed no morphological changes after 48 h of lead exposure at all concentrations compared to unexposed control SCs. These findings were confirmed by the fluorescence analysis of the actin cytoskeleton that revealed a well-developed network of stress fibres composed of actin filaments both in lead-exposed and unexposed SCs, consistent with the findings reported by Iida et al, 2003; lead exposure at all concentrations did not alter the distribution of vimentin filaments compared to unexposed SCs. In addition, the MTT assay showed a significant increase in cell viability in SCs exposed to all concentrations of lead compared to unexposed SCs; similarly, Razani-boroujerdi et al, 1999, demonstrated an increase in lymphocyte proliferation upon lead exposure, probably due to the progression of pre-existing G1 cells into the cell cycle. In our study, this increase in SC proliferation was supported by an increase in p38 phosphorylation, a typical MAPK target activated by cellular stress (Zhang and Liu, 2002); however, no alteration in the phosphorylation status of ERK1/2 and JNK was observed (data not shown). Moreover, lead exposure increased Akt activation (indicated by an increase in Akt mRNA and phospho-Akt levels). Similarly, Eckers and Klotz (2009) have reported that exposure to heavy metals activate the PI3K/Akt signalling cascade in mammalian cells, thereby revealing the insulin-mimetic effects of these heavy metals.

In addition, in our study, SC exposure to subtoxic lead concentrations significantly increased the gene expression of mTOR, a potential downstream effector of the PI3K pathway that regulates cell death signalling (Chen et al, 1995), indicating that SC monolayers rely on mTOR expression for survival under stress conditions.

The simultaneous increase in cell proliferation and the activation of p38/MAPK and PI3K/Akt/mTOR pathways also could represent the preliminary phases of replicative senescence, according to Eckers

and Klotz (2009), who describe heavy metal stress as a pro-senescence factor. Replicative senescence is a form of irreversible growth arrest associated with the exhaustion of replicative potential, preceded by an initial phase of hyperproliferation. This senescence has been demonstrated during oncogenic transformation in multiple human and mouse cancer models, and acts as an initial barrier to cancer development *in vivo*; it is characterised by the activation of p38/MAPK and PI3K/Akt/mTOR pathways (Xu et al, 2014). Therefore, lead-exposed SCs in our study were found to respond to stress in various ways ranging from the activation of survival pathways to the eventual elimination of damaged cells that is expected to alter spermatogenesis.

Moreover, we observed that lead exposure reduces the levels of AMH and inhibin B both in the supernatants and cell extracts; it also attenuates FSH-r integrity, as observed by the reduced FSH-r gene expression and 17-β-oestradiol secretion, indicating the alteration of SC function.

5. Conclusion

Our data indicate that SCs in higher order mammals are sensitive to subtoxic lead exposures. Although SC morphology and viability were not significantly affected in our experiments, we demonstrated for the first time that subtoxic lead exposures alter the functioning of neonatal SCs by decreasing the synthesis and secretion of AMH, inhibin B, and 17-β-oestradiol after FSH/testosterone stimulation. Moreover, it increased cell proliferation by attenuating apoptosis through the activation of p38/MAPK and PI3K/Akt/mTOR signalling pathways, indicating the attempt of SC monolayers to survive under stress conditions; this could represent the preliminary phase of heavy metal-induced replicative senescence. These findings highlight the necessity of major occupational health surveillance programs to assess the adverse effects of subtoxic lead exposure on SCs before the onset of irreversible impairment in spermatogenesis.

Nevertheless, further studies are warranted to better understand the chronic consequences of lead exposure.

Acknowledgements

This study was supported by Altucell Inc., 3 Astor Court, Dix Hills, NY, USA and the Inter-University Consortium for Organ Transplantation, Rome, Italy.

Author Contributions: M. F. isolated the SCs, performed lead exposure studies, discussed the data, and wrote the manuscript. A. I., L. C. and B. C. performed lead exposure studies, RT-PCR, and 17-β-oestradiol assay; C. R. and B. M. supervised the experiments and critically revised the manuscript. A. M. C. performed experiments by ELISA. C. M. isolated the SCs. D. M. and N. C. analysed and interpreted the data. L. G. and M. L. supervised the research and edited the manuscript. All authors agreed on the results obtained and the final version of the manuscript.

Competing financial interests

The authors declare no competing financial interests.

Figure legends

Fig. 1. ***In vitro*** **characterisation of cultured neonatal porcine SC monolayers by fluorescence microscopy.** (a) AMH, (b) 3β-HSD, and (c) ASMA immunostaining; secondary antibodies are conjugated with Alexa Fluor 488 (green), and nuclei are counterstained with DAPI (blue). The images are representative of three separate experiments.

Fig. 2. *In vitro* morphological characterization of cultured neonatal porcine SC monolayers (a) Vimentin immunostaining in unexposed control SC monolayers (a) and SC monolayers exposed to (b) 10, (c) 20, and (d) 40 μM of lead; secondary antibody is conjugated with Alexa Fluor 488 (green), and nuclei are counterstained with DAPI (blue). Phalloidin staining in unexposed control SC monolayers (e) and SC monolayers exposed to (f) 10, (g) 20, and (h) 40 μM of lead; phalloidin is conjugated with Alexa Fluor 555 (red), and nuclei are counterstained with DAPI (blue). Light microscope images of unexposed control SCs (i) and SCs exposed to (l) 10, (m) 20, and (n) 40 μM of lead. The images are representative of three separate experiments.

Fig. 3. FSH-r integrity. α-aromatase activity assessed by the levels of 17-β-oestradiol under basal conditions (black bars), and under FSH stimulation (grey bars) in the culture supernatant. Data represent the mean±S.E.M. (*$p<0.05$ and **$p<0.001$) of three independent experiments, each performed in triplicate.

Fig. 4. SC functioning. Inhibin B and AMH secretion in (a) the culture supernatant and (b) cell extracts. Data represent the mean±S.E.M. (*$p<0.05$ and **$p<0.001$) of three independent experiments, each performed in triplicate.

Fig. 5. WB analysis. (a) Immunoblots of phospho-p38, p38, phospho-Akt, Akt, and actin. (b) Densitometric analysis of the protein bands of phospho-p38, p38, phospho-Akt, and Akt. Data represent the mean±S.E.M. (*$p<0.05$ and **$p<0.001$) of three independent experiments, each performed in triplicate.

Fig. 6. RT-PCR analysis of FSH-r, inhibin B, AMH, Akt, and mTOR gene expression. Data represent the mean±S.E.M. (*p<0.05 and **p<0.001) of three independent experiments, each performed in triplicate.

Fig. 7. Number of cells and cytotoxicity. (a) Cell numbers were evaluated by the trypan blue exclusion assay. (b) Cytotoxicity was evaluated using the MTT assay. Data represent the mean±S.E.M. (*p<0.05 and **p<0.001) of three independent experiments, each performed in triplicate.

References

Adhikari, N., Sinha, N., Saxena, D.K., 2000. Effect of lead on Sertoli–germ cell coculture of rat. Toxicology Letters 116, 45–49.

Baroni, T., Lilli, C., Bellucci, C., Luca, G., Mancuso, F., Fallarino, F., Falabella, G., Arato, I., Calvitti, M., Marinucci, L., Muzi, G., Dell'Omo, M., Gambelunghe, A., Bodo, M., 2015. In vitro cadmium effects on ECM gene expression in human bronchial epithelial cells. Cytokine, 72: 9-16.

Batarseh, L. I., WM. J., Brabec M. J., 1986. Effect of lead acetate on sertoli cell lactate production and protein synthesis in vitro. Cell Biology and Toxicology, 2, 283-291.

Benjelloun, M., Tarrass, F., Hachim, K., Medkouri, G., Benghanem, M.G., Ramdani, B., 2007. Chronic lead poisoning: a "forgotten" cause of renal disease. Saudi J Kidney Dis Transpl. 18, 83-86.

Bodo M., Balloni S., Lumare E., Bacci M., Calvitti M., Dell'Omo M., Murgia N., Marinucci L., 2010. Effects of sub-toxic Cadmium concentrations on bone gene expression program: Results of an in vitro study. Toxicology in Vitro 24, 1670-1680.

Bradford, M.M., 1976. A rapid and sensitive method for the quantitation of microgram quantities of protein utilizing the principle of protein-dye binding. Anal Biochem 72, 248-254.

Chen, J., Zheng, X.F., Brown, E.J., Schreiber S.L., 1995. Identification of an 11-kDa FKBP12 rapamycin-binding domain within the 289-kDa FKBP12-rapamycin-associated protein and characterization of a critical serine residue. Proc. Natl. Acad. Sci. U. S. A. 92, 4947–4951.

Dietert, R. R., Piepenbrink M. S., 2006, Lead and immune function. Crit Rev Toxicol. 36, 359-385. DOI:10.1080/10408440500534297.

Dowling, R.J.O., Topisirovic, I., Fonseca, B.D., Sonenberg, N, 2010. Dissecting the role of mTOR: Lessons from mTOR inhibitors. Biochimica et Biophysica Acta 1804, 433–439.

Eckers, A., Klotz, L.O., 2009. Heavy metal ion-induced insulin-mimetic signaling. Redox Rep. 14, 141-146.

França, L.R., Hess, R.A, Dufour, J.M., Hofmann, M.C., Griswold, M.D., 2016. The Sertoli cell: one hundred fifty years of beauty and plasticity. Andrology 4, 189–212.

Gidlow, D. A., 2004. Lead toxicity. Occup. Med. (Lond.) 54, 76–81.

Giovagnoli, S., Mancuso, F., Vannini, S., Calvitti, M., Piroddi, M., Pietrella, D., Arato, I., Falabella, G., Galli, F., Moretti, M., Neri, L. M., Bodo, M., Capitani, S., Cameron, D. F., Ricci, M., Luca, G., Calafiore, R., 2014. Microparticle-loaded neonatal porcine Sertoli cells for cell-based therapeutic and drug delivery system. Journal of Controlled Release 192, 249–261.

Li, Z., Liu, X., Wanga, L., Wang, Y., Du, C., Xu, S., Zhang, Y., Wang, C., Yang, C., 2016. The role of PGC-1a and MRP1 in lead-induced mitochondrial toxicity in testicular Sertoli cells. Toxicology 355–356: 39–48. DOI.org/10.1016/j.tox.2016.05.016

Luca, G., Calvitti, M., Nastruzzi, C., Bilancetti, L., Becchetti, E., Angeletti, G., Mancuso, F., Calafiore, R., 2007. Encapsulation, in vitro characterization, and in vivo biocompatibility of Sertoli cells in alginate-based microcapsules.Tissue Eng. 13, 641-648.

Luca, G., Mancuso, F., Calvitti, M., Arato, I., Falabella, G., Bufalari, A., De Monte, V., Tresoldi, E., Nastruzzi, C., Basta, G., Fallarino, F., Lilli, C., Bellucci, C., Baroni, T., Aglietti, M. C., Giovagnoli, S., Cameron, D.F., Bodo, M., Calafiore, R., 2015. Long-term stability, functional competence,and safety of microencapsulated specificpathogen-free neonatal porcine Sertoli cells:a potential product for cell transplant therapy. Xenotransplantation. 22, 273-283. DOI: 10.1111/xen.12175

Iida, H., Kazue, M., Doiguchi, M., Mori, T., Yamada, F., 2003. Bisphenol A-induced apoptosis of cultured rat Sertoli cells. Reproduct. Toxicol. 17, 457–464.

Luca, G., Lilli, C., Bellucci, C., Mancuso, F., Calvitti, M., Arato, I., Falabella, G., Giovagnoli, S., Aglietti, M. C., Lumare, A., Muzi, G., Calafiore, R., Bodo, M., 2013. Toxicity of cadmium on Sertoli cell functional competence: an in vitro study. J Biol Regul Homeost Agents 27, 805-816.

Marinucci, L., Bodo, M., Balloni, S., Locci, P., Baroni, T., 2014. Sub-toxic nicotine concentrations affect extracellular matrix and growth factor signaling gene expressions in human osteoblasts. J. Cell. Physiol. 229, 2038-2048.

Mason, L. H., Harp, J. P., Han, D. Y., 2014. Lead Neurotoxicity: Neuropsychological effects of lead toxicity. BioMed Research International Volume, Article ID 840547, DOI.org/10.1155/2014/840547.

Monsees, T.K. Franz, M., Gebhardt S., Winterstein, U. Schill W.B., Hayatpour, J. 2000. Sertoli cells as a target for reproductive hazards Andrologia 32, 239–246.

Obrist, D., Agnan, Y., Jiskra, M., Olson, C. L., Colegrove D. P., Hueber J., Moore C. W., Sonke, J. E., Helmig, D., 2017. Tundra uptake of atmospheric elemental mercury drives Arctic mercury pollution. Nature. 547. 201-204. doi: 10.1038/nature22997.

Occupational Safety and Health Administration. OSHA 3142-12R. 2004

Pant, N., Kumar, G., Upadhyay, A.D., Patel, D.K., Gupta, Y.K., Chaturvedi, P.K., 2014. Reproductive toxicity of lead, cadmium, and phthalate exposure in men. Environ. Sci. Pollut. Res. Int. 21, 11066–11074.

Razani-boroujerdi, S., Edwards, B. and Sopori, M.L., 1999. Lead Stimulates Lymphocyte Proliferation Through Enhanced T Cell-B Cell Interaction. The Journal of Pharmacology and Experimental therapeutics. 288, 714–719.

Vaseem, H., Singh, V. K., Singh, M. P., 2017. Heavy metal pollution due to coal washery effluent and its decontamination using a macrofungus, Pleurotus ostreatus. Ecotoxicol Environ Saf. 145, 42-49. doi: 10.1016/j.ecoenv.2017.07.001.

Vaziri, N. D., 2008 Mechanisms of lead-induced hypertension and cardiovascular disease Am J Physiol Heart Circ Physiol. 295, H454–H465. DOI: 10.1152/ajpheart.00158.2008.

Vigeh, M., Derek R., Smith, D.R., Hsu, P.C., 2011. How does lead induce male infertility? Iran J Reprod Med. 9, 1–8.

Wirth, J. J. and Mijal, R. S., 2010. Adverse Effects of Low Level Heavy Metal Exposure on Male Reproductive Function. Systems Biology in Reproductive Medicin 56, 147-167.

Wang, C., Zhang, Y., Liang, J., Shan, G., Wang, Y., Shi, Q., 2006. Impacts of ascorbic acid and thiamine supplementation at different concentrations on lead toxicity in testis. Clin. Chim. Acta 370, 82–88.

Xu, Y., Li, N., Xiang, R., Sun, P., 2014. Emerging roles of the p38 MAPK and PI3K/AKT/mTOR pathways in oncogene-induced senescence. Trends in Biochemical Sciences, 39, 268-276.

Zhang, W., Tu, Liu H., 2002. MAPK signal pathways in the regulation of cell proliferation in mammalian cells. Cell Research 12, 9-18.

Zhang, W., Shen, X.., Wan, C, Zhao, Q., Zhang, L., Zhou, Q., Deng, L., 2012. Effects of insulin and insulin-like growth factor 1 on osteoblast proliferation and differentiation: differential signalling via Akt and ERK. Cell Biochem Funct. 30, 297-302.

Highlights:

1. Exposure of purified pig prepubertal SC to sub-toxic Pb concentrations was performed;

2. Inhibin B and anti-Mullerian hormone (AMH) mRNAs and proteins were decreased***;***

3. FSH-r integrity, in terms of 17-β-estradiol production, was decreased under FSH stimulation***;***

4. We observed an increase of AKT and mTOR mRNAs, p38 and Akt phosphorylation ratio***;***

5. Pb-related toxicity on SC, even at low concentrations, is expected to alter spermatogenesis.